iTRAQ-based proteomic technique provides insight into salt stress responsive proteins in Apocyni Veneti Folium (Apocynum venetum L.)

Cuihua Chen¹, Chengcheng Wang¹, Zixiu Liu¹, Zhichen Cai¹, Yujiao Hua¹, Yuqi Mei¹, Lifang Wei¹, and Xunhong Liu¹

¹Nanjing University of Chinese Medicine

April 28, 2020

Abstract

Soil salinity is a major abiotic stress that limits plant growth and productivity. Understanding the mechanisms of plant salinity tolerance can facilitate engineering for quality improvement. Apocynum venetum L. exhibits tolerance to salinity. Due to the lack of a genomic database, RNA-seq based transcriptomics and isobaric tag for relative and absolute quantitation (iTRAQ) based proteomic profiles of Apocyni Veneti Folium (AVF) exposed to four levels of salt treatments were performed. A total of 143, 162 and 167 differentially expressed proteins (DEPs) were found between salt-treated AVF compared with control, respectively. They were mainly involved in carbohydrate and energy metabolism, biosynthesis of metabolites and signal transduction. Furthermore, results showed that carbon and nitrogen metabolisms were altered under salt stress; low and moderate levels of salt stress enhanced photosynthetic functions and ramped up carbohydrate metabolism. However, severe salt stress depressed biosynthesis of secondary metabolites, consistent with the metabolomics results. In conclusion, the protein profiles combined with transcriptomics and metabolomics indicate that halophyte uses a multipronged approach to overcome salt stress, and provides some novel information for revealing the mechanisms of adaption and quality formation of this herbal medicine.

iTRAQ-based proteomic technique provides insight into salt stress responsive proteins in Apocyni Veneti Folium (*Apocynum vene*tumL.)

Cuihua Chen 1, Chengcheng Wang 1, Zixiu Liu 1, Zhichen Cai 1, Yujiao Hua 1, Yuqi Mei 1, Lifang Wei 1, Xunhong Liu 1,2,3,*

¹ College of Pharmacy, Nanjing University of Chinese Medicine, Nanjing 210023, China;

² Collaborative Innovation Center of Chinese Medicinal Resources Industrialization, Nanjing 210023, China;

³ National and Local Collaborative Engineering Center of Chinese Medicinal Resources Industrialization and Formulae Innovative Medicine, Nanjing 210023, China.

*Correspondence: liuxunh1959@163.com.

Running title: Proteomics reveals quality formation mechanism

ABSTRACT

Soil salinity is a major abiotic stress that limits plant growth and productivity. Understanding the mechanisms of plant salinity tolerance can facilitate engineering for quality improvement. *Apocynum venetum* L. exhibits tolerance to salinity. Due to the lack of a genomic database, RNA-seq based transcriptomics and isobaric tag for relative and absolute quantitation (iTRAQ) based proteomic profiles of Apocyni Veneti Folium (AVF) exposed to four levels of salt treatments were performed. A total of 143, 162 and 167 differentially expressed proteins (DEPs) were found between salt-treated AVF compared with control, respectively. They were mainly involved in carbohydrate and energy metabolism, biosynthesis of metabolites and signal transduction. Furthermore, results showed that carbon and nitrogen metabolisms were altered under salt stress; low and moderate levels of salt stress enhanced photosynthetic functions and ramped up carbohydrate metabolism. However, severe salt stress depressed biosynthesis of secondary metabolites, consistent with the metabolomics results. In conclusion, the protein profiles combined with transcriptomics and metabolomics indicate that halophyte uses a multipronged approach to overcome salt stress, and provides some novel information for revealing the mechanisms of adaption and quality formation of this herbal medicine.

Keywords:

Apocyni Veneti Folium; correlate analysis; halophyte; proteomics; salt tolerance

INTRODUCTION

Soil salinity is a prevalent abiotic stress. High levels of salt can cause metabolism disorders, osmotic stress, ion imbalance, mineral nutrient deficiency, water uptake interference, oxidative damage, toxic ions accumulation and eventually growth inhibition (Pi *et al.*, 2018; Yang *et al.*, 2013). To reduce these detrimental effects under salt stress, evidence shows that plants have evolved complex physiological and molecular responses allowing for adaptation, including selection of ion uptake and exclusion, compartmentalization of Na⁺ in vacuoles, synthesis of compatible solutes, adjustment of photosynthesis, detoxification of reactive oxygen species (ROS) and regulation of specific protein expressions (Zhang *et al.*, 2012). Moreover, halophytes have developed unique structures that allow them to grow under severe salt stress conditions (Chen *et al.*, 2018). An improved understanding of molecular responses to NaCl treatment may therefore facilitate the development of plants with increased tolerance to salt stress.

Apocynum venetum L. (AVL), a well-known medicinal halophyte, has attracted much attention in terms of its antioxidant properties. Modern pharmacological studies have demonstrated that Apocyni Veneti Folium (AVF) has several pharmacological functions, such as anti-hypertension, anti-depressant and hepatoprotection (Xie *et al.*, 2012). Although AVL exhibits a high physiological plasticity for salt tolerance, its growth is affected by salt stress (Chen *et al.*, 2018; Xie*et al.*, 2012). Our previous studies have shown that this medicinal herb can tolerate 300 mM NaCl treatment, under which a total of 51 metabolites exhibited significant alteration (Chen *et al.*, 2019b). Although these salt-responsive metabolites are important, plant salt tolerance is controlled by sophisticated signaling and metabolic networks. Therefore, it is necessary to establish a truly meaningful protocol to effectively and systematically reveal the mechanism of salt tolerance and quality formation of AVF.

High-throughput transcriptomics of identifying salt-responsive genes and molecular regulatory pathways has contributed to our understanding of salinity stress in species including Arabidopsis (Stanley Kim *et al.*, 2005), *Jerusalem artichoke* (Zhang *et al.*, 2018) and soybean (Liu *et al.*, 2019). However, the transcriptome data may not correlate well with the results from proteomic analysis because mRNA levels are not always correlated to those of corresponding proteins due in part to post-transcriptional and post-translational modifications. Previous evidence showed that only poor or moderate correlation between the two levels of expression was found in species (Mooney *et al.*, 2006). Proteomic analysis is a tool that facilitates the study of global protein expression and provides a large amount of information about the

individual proteins involved in specific biological responses. Proteomic profiles have been built for different species, including Arabidopsis (Jiang *et al.*, 2007), sugar beet (Wu *et al.*, 2018), *Aeluropus lagopoides* (Sobhanian *et al.*, 2010), soybean (Piet *al.*, 2016), *Salicornia europaea* (Wang *et al.*, 2009), sesame (Zhang *et al.*, 2019), *Panax ginseng* (Kim*et al.*, 2019) as well as spinach (Li *et al.*, 2019). Additionally, isobaric tags for relative and absolute quantification (iTRAQ) have become a powerful tool in quantitative proteomics, especially for hydrophobic and low-abundant proteins in cells and organelles under different environmental conditions (de Abreu *et al.*, 2014; Liu *et al.*, 2014b; Wang *et al.*, 2013; Wang*et al.*, 2019), such as, salt-stressed *Kandelia candel*(Wang *et al.*, 2013), *Jerusalem artichoke* (Zhang *et al.*, 2018) and Arabidopsis (Pu *et al.*, 2019), drought-stressed cassava (Ding *et al.*, 2019), virus-infected tobacco (Das *et al.*, 2019) and heavy-metal-stressed *Typha angustifolia* (Bah*et al.*, 2010). However, in spite of the progress underlying salt-tolerant mechanisms based on physiology and metabolomics (Chen *et al.*, 2019b; Chen *et al.*, 2018), a comprehensive description of the proteome changes and gene transcription is lacking.

In this present study, we combined transcriptomics based on RNA-seq technology with proteomics based on iTRAQ platform, and then integrated the results with previous study on metabolomics and physiology (Chen*et al.*, 2019b). The generalized workflow was shown in Fig. 1. On the basis of bioinformatics analysis, 300 differentially expressed proteins (DEPs) were categorized and analyzed. Then, quantitative reverse transcriptase-polymerase chain reaction (qRT-PCR) results and transcriptomics altogether were used to validate the expression levels between transcripts and their corresponding proteins. Gaining knowledge of salt tolerance in AVF from integrated transcriptomics, proteomics and metabolomics provides insights into the molecular basis of plant salt tolerance, which ultimately leads to quality improvement.

MATERIALS AND METHODS

Plant material and salt treatment

Salt stress experiments have been described in detail in our previous articles (Chen *et al.*, 2019b; Chen *et al.*, 2018). Briefly, the experiment was carried out in the shelter covered by a transparent film that blocked rainwater, while other conditions were similar to the open-air environment in Nanjing University of Chinese Medicine. The main roots of AVL (two years old and originated from the same plant) were planted in pots filled with 25 kg of soil. The parameters of soil were as follows: texture, loam; organic carbon, 36.6 g kg⁻¹; cation exchange capacity, 17.0 cmol(+) kg⁻¹; pH, 5.0. Salt stress tests were conducted when AVL was about 30 cm height. Four groups were exposed to different levels of salt treatment, 0 (control, watering), 100 (low stress), 200 (moderate stress) and 300 (high stress) mM NaCl, respectively. All groups were designed with 9 replicates and 3 pots per replicate by pouring 2 L of solution. NaCl concentrations increased gradually by 50 mM every four days to reduce osmotic shock until the designated concentration was reached and the treatments were lasted for 6 times (20 days). After 12 h of the last salt treatments, leaves were harvested. After being quick frozen in liquid nitrogen, these leaves were transferred to a -80 °C refrigerator for storage.

Transcriptome analysis

Total RNA was extracted from 100 mg leaves according to the manufacture's protocol using RNAprep Qubit RNA kit and Agilent Technologies 2100 Bioanalyzer. The RNA integrity and quality was confirmed by a NanoDrop ND-1000[®] spectrophotometer (GE Healthcare) and electrophoresed in 1 % agarose gel. Then, poly(A) mRNA was purified with Oligod(dT) beads and fragmented. After synthetization of first-strand cDNA using reverse transcriptase and random primers, second-strand cDNA was synthesized using DNA polymerase I. Four groups were subjected to end repair and addition of a single A base and ligation with adapters. Suitable fragments were amplified through PCR to create a library for sequencing using Illumina HiSeqTM2500. No reference genomes were used for AVF transcriptomic analysis. Clean reads were obtained by ngsQCToolkit-2.3.32 for purification and filtration of low-quality sequences of the raw data. High-quality reads were assembled with Trinity software to construct a unigene library after further filtration. The unigenes showed an average ratio-fold change $|log_2FC|$ [?]1 and FDR[?]0.05 were confidently considered as differentially expression genes (DEGs). The raw data of transcriptomes converting to proteome library

Protein extraction, digestion, iTRAQ labeling and strong cation exchange

To ensure the ability to conduct statistical analyses, two biological replicates (12 plants per replicate) were used for the iTRAQ-based quantitative proteomic analysis. The procedure for protein extraction was modified from the phenol method (Li *et al.*, 2015; Wang*et al.*, 2013). In short, samples of AVF (about 100 mg) were vortexed with 10 mL extraction buffer. The extraction was performed under shaking, followed by centrifugation. The phenol phase transferred was re-extracted under the same conditions; this step was repeated once more. After precipitation and resuspension, proteins were rinsed, and then transferred into a new tube and centrifuged. Protein pellets were dissolved in RIPA buffer and centrifuged. Finally, the pellets were air-dried and ready for use. The protein concentrations were determined using the BCA method.

Proteins were digested according to the FASP method (Hua *et al.*, 2016; Lan *et al.*, 2011; Wang *et al.*, 2013). iTRAQ labeling was performed according to the manufacturer's instructions (Applied Biosystems). The control samples' replicates were labeled with tags 113 and117, and the salt-treated labeled with tags 114 and 118 (100 mM salt treatment), tags 115 and 119 (200 mM salt treatment), tags 116 and 121 (300 mM salt treatment), respectively. After labeling, individual iTRAQ 8-plex samples were mixed and diluted into 0.1% trifluoricacetic acid, followed by loading on a C₁₈ reverse phase mini-column. After washing and elution, the eluates were dried down and dissolved by strong cation exchange (SCX) solvent A (25% v/v acetonitrile, 10 mM ammonium formate, pH 2.8). The peptides were eluted by 20 mM HCOONH₄ (pH 10) and 20 mM HCOONH₄ and 80% acetonitrile (pH 10) for phase B, and UV wavelength was set at 214 nm and 280 nm with a flow rate at 0.2 mL min⁻¹.

Tandem mass spectrometry analysis

The fractionated samples were lyophilized to remove acetonitrile and resuspended in 5% acetonitrile and 0.1% formic acid, and then centrifuged. The nano LC–MS/MS was carried out using a Thermo Scientific Q Exactive. The peptide mixture was loaded on an Acclaim PepMap RSLC C₁₈ (75 μ m × 150 mm, 2 μ m, 100 Å). 0.1% formic acid was used as buffer A and 80% acetonitrile/0.1% formic acid as buffer B. The peptides were eluted at a flow rate of 0.3 mL min⁻¹ with a gradient (B%): 0–4% for 5 min, 4%–50% from 5 to 45 min, 50%–90% from 45 to 50 min, and 4% for 15 min.

MS data analysis and protein identification

MS data were performed using Proteome Discoverer 1.3 software. To increase the confidence level, proteins with an iTRAQ ratio higher than 20 or less than 0.05, or the absolute value of coefficient of variation (C.V.) larger than 0.5 were not considered as quantified (Zhang *et al.*, 2019). DEPs were selected based on the following criteria: proteins in which the mean ratio corresponding to the protein reporter ion intensity originating from salt-treated protein samples with respect to fully control protein samples had an average ratio-fold change [?]1.5 or [?]0.67, respectively; p [?] 0.05 (Zhao *et al.*, 2016).

Bioinformatics analysis

Open reading frame of AVF obtained from the sequences of the transcriptome was established into a protein database. Then, the sequences of protein database was compared with the databases of Uniprot, Swissprot, NCBI, NR, Gene Ontology (GO), Kyoto Encyclopedia of Genes and Genomes (KEGG) and Clusters of Orthologous Groups of proteins (COG). GO analysis of proteins was carried out using QuickGO software which was performed using BLASTp search against Uniprot to find the ID of proteins and then annotate them, generating molecular function, biological process, and cellular component information. KEGG database was used to take advantage of the current knowledge of biochemical pathways and other types of molecular interactions (Hua *et al.*, 2016). DEPs were classified according to GO, KEGG and STRING to predict functions, significant pathways and protein-protein interaction.

Total RNA extraction and qRT-PCR analysis

To examine relationships between mRNA expression and protein abundance under salt stress, the relative transcript level of nine salt-responsive proteins was examined by qRT-PCR. Briefly, total RNA was extracted from salt-treated and control AVF by plant RNA kit (R6827-01, Omega Bio-Tek), and cDNA was reverse transcribed from 1 µg of total RNA using a first strand cDNA synthesis kit (Yeasen). Gene-specific primers used for qRT-PCR were designed using Primer 5 software according to cDNA sequences obtained from the AVF RNA-seq (Table S1). The truncated beta-actin gene was used as an endogenous control for normalization. The PCR reaction was carried out in a 20 µL volume containing 10 µL 2 ×Hieff[®] qPCR SYBR Green Master Mix reagent (Yeasen), 2 µL template cDNA, 0.4 µL of each primers and 7.2 µL sterilized water with the following reaction conditions: 95 °C for 5 min; followed by 40 cycles of 95 °C for 10 s; 60 °C for 30 s. Three biological replicates (12 plants per replicate) were used. Relative gene expression was calculated using the formula 2^{-[?][?]Ct} (Li *et al.*, 2015).

Correlation between DEGs and DEPs

The correlation between transcripts and protein abundance in each salt treatment compared to control was achieved by SPSS 14.0 software.

Data analysis

Statistical analyses of data among groups were performed using Student's t-test at a 0.05 level. Statistical analysis was performed by one-way analysis of variance. Data are presented as means +-SD of three replicates.

RESULTS

iTRAQ primary data analysis and protein detection

Based on the iTRAQ analysis, a total of 28775 spectra were generated from the iTRAQ experiment. By matching to known spectra, 8087 unique peptides and 4344 proteins were detected. Summary of the iTRAQ information was shown in Fig. 2. There were 13977, 24024, 3478, and 509 peptides with 4–10, 11–20, 21–30, and more than 30 peptide length, respectively (Fig. 2A). Isoelectric point of the majority identified protein was between 4.5and 10 (Fig. 2B), and over 84.9% of the proteins included at least two peptides (Fig. 2C). Mass distribution of the identified protein species showed that more than half of them were 20-80 kDa (Fig. 2D). In addition, sequence coverage of the majority of identified protein species was less than 30% (Fig. 2E).

Identification and functional classification of DEPs

Based on the criteria mentioned in the experimental section, 143, 162 and 167 DEPs were found in comparison between salt-stressed samples and control (Fig. 3A), of which 40 were shared in three comparisons. In detail, there were 85, 110 and 99 up-regulated and 58, 52 and 68 down-regulated proteins for low, moderate and high level of salt treatments versus control, respectively (Fig. 3B).

All salt-responsive DEPs in different levels of salt stress were classified by GO annotation software into three functional groups: molecular function, biological process and cellular component (Fig. 3C). On the basis of biological process analysis, most of the DEPs were found to be related to small molecule metabolic process, biosynthetic process, response to stress, carbohydrate metabolic process, translation and catabolic process. In addition, most of the annotated molecular functions were found to be related to ion binding, oxidoreductase activity, structural constituent of ribosome and hydrolase activity. In the category of cellular component, thylakoid, intracellular, plastid and ribosome were the most represented.

KEGG and STRING analysis of DEPs

The KEGG analysis demonstrated that metabolic pathways, biosynthesis of secondary metabolites, photosynthesis, biosynthesis of antibiotics, ribosome were prominently affected. A total of 300 proteins participated in 152 pathways. E.g., 32, 44 and 42 DEPs were involved in metabolic pathways for the low, moderate and high level of salt stress, respectively; 18, 27 and 33 DEPs were involved in biosynthesis of secondary metabolites, respectively, followed by 9, 7 and 5 DEPs related to photosynthesis, respectively (Fig. 4). Obviously, DEPs were involved in more pathways with the increasing levels of salt treatments.

The function of proteins is vital to cells. To predict the protein interactions, functional relations and networks among DEPs using STRING software (Fig. 5). It can be observed that extensive interactions were found amongst ribosomal proteins (RPs) and heat shock proteins (HSPs), or between HSPs and other proteins with the enhanced levels of salt stress. These results indicate that RPs and HSPs probably play roles in protecting protein functions under salt stress conditions.

Shared DEPs of AVF in response to salt stress

The relative abundance and functional properties of a list of 40 DEPs shared in three comparisons was given in Fig. 6A. The main molecular functions were ion binding, followed by oxidoreductase activity (Fig. 6B), and the main biological processes were related to response to stress, followed by carbohydrate metabolic process (Fig. 6C). KEGG pathways showed that photosynthesis, ribosome, nitrogen metabolism, biosynthesis of secondary metabolites, carbon metabolism and phenylpropanoid biosynthesis, were altered under salt tolerance (Fig. 6D). In addition, the STRING analysis revealed that shared DEPs, such as HSPs and RPs were interacted in response to salinity (Fig. 6E). Taken together, shared DEPs in three comparisons probably play important roles role in improving AVF salt tolerance.

Transcriptional analysis by qRT-PCR

Nine DEPs, selected from several enriched pathways, such as peroxisome, phenylpropanoid biosynthesis, photosynthesis, ribosome, Foxo signaling pathway and plant-pathogen interaction, were examined between mRNA expression level and protein abundance by qRT-PCR (Fig. 7). Results showed the expressions levels of six genes, Tr_AVENL_20218 (uncharacterized protein), Tr_AVENL_23089 (ATP synthase subunit delta, chloroplastic), Tr_AVENL_3558 (ruBisCO large subunit-binding protein subunit beta, CPN60B), Tr_AVENL_4882 (catalase isozyme 1-like, CAT), Tr_AVENL_23055 (pathogenesis related protein, PRH) and Tr_AVENL_972 (dehydrin 1) were consistent with the corresponding DEPs abundance, indicating that these proteins were regulated at the transcriptional level. While, the transcript levels of the remaining three genes (Tr_AVENL_17965, Tr_AVENL_25878 and Tr_AVENL_27306) were inconsistent with the protein expression levels. In addition, the result of qRT-PCR was consistent with that of transcriptome with the exception of Tr_AVENL_20218 and Tr_AVENL_23089 (Fig. 8). Specifically, the qRT-PCR result of Tr_AVENL_20218 was up-regulated while it was down-regulated in transcriptome under low level of salt stress. Similarly, up-regulated level of Tr_AVENL_23089 in qRT-PCR result under moderate and high levels of salt stress was found to be inconsistent with the transcriptome analysis.

Correlation analysis between transcripts and proteins

We generated RNA-seq data from the same samples. After further identification DEGs under salt treatments by comparing with control, a total of 807, 1512 and 1258 DEGs were obtained in three comparisons, respectively. 23, 16 and 11 DEGs/DEPs showed significant correlation in gene expression and protein levels under low, moderate and high levels of salt stress compared to the control, respectively, showing increasing correlations (0.29, 0.57 and 0.63, respectively) (Fig. 9A-C). Fig. 9D revealed a weak correlation (R = 0.49) in 49 DEGs/DEPs found in the salt-stressed AVF in comparison with control , and four DEPs shared in three comparisons, including dehydrin 1, annexin, PRH and prolyl oligopeptidase (POP) (Fig. 6A), were contained in these significant correlated DEGs/DEPs. Therefore, these DEPs may play active roles role in AVF tolerance to salt stress.

DISCUSSION

Halophytes can complete their life cycle at salinities above 200 mM NaCl (Flowers, 2004). Meanwhile, molecular mechanisms of halophytes in response to salt stress revealed that some plants evolved specific salt-tolerant mechanisms (Wang *et al.*, 2009). Our previous study on metabolomics analysis (Chen *et al.*, 2019b) indicated that AVF exposure to low level of salt stress had the strongest ability to adapt to salt shock, followed by the moderate level one, and the summarized data was shown in Fig. S1. In this study, combined with transcriptomics, proteomics and metabolomics, we focused our analysis on the DEPs related to carbohydrate and energy metabolism, lipid and amino acid metabolism, biosynthesis of secondary metabolites, signal transduction, transcription, translation, as well as protein folding and degradation and provide insight into AVF salt tolerance (Table S2).

Proteins related to carbohydrate metabolism

In many plants, proteins associated with carbohydrate metabolism altered expression patterns severely under salt stress (Yang et al., 2013; Zhang et al., 2012). In our study, a large proportion of DEPs involved in carbohydrate metabolism, such as glycolysis/gluconeogenesis, citrate cycle, starch and sucrose metabolism, pentose phosphate pathway and carbon fixation in photosynthetic organisms, was altered the abundance; many of them were up-regulated, such as beta-glucosidase 44-like (BGLU), fructose-bisphosphate aldolases (FBAs), triosephosphate isomerase (TPI), two malate dehydrogenases (MDH), phosphoglycerate kinase (PGK) and glyceraldehyde 3-phosphate dehydrogenase (GAPDH), pyruvate kinase (PK), beta-galactosidase 1 (BGAL1), alpha-amylase (AMY), two chitinase family proteins, serine-glyoxylate aminotransferase (sgaA), glucose-1phosphate adenvivitransferase (APS) and UN (gi/661880779). Specifically, BGLU is a key enzyme in the cellulose hydrolysis process causing abscisic acid-glucose conjugate hydrolysis (Yang et al., 2013). The activity of an extracellular BGLU was up-regulated under moderate level of salt stress, which was consistent with the reports that it was highly induced in barley (Dietz et al., 2000) under salt stress. Furthermore, the overexpression of BGLU genes regulated endogenous abscisic acid (ABA) levels during the development of watermelons under drought stress (Li et al., 2012). Similarly, the relative abundance of two FBAs was accumulated under high level of salt stress. Similar results were found in heat-stressed alfalfa seeds (Li et al. , 2013) and grape leaves (Liu et al., 2014b) and NaCl-stressed sugar beet (Yang et al., 2013). Chloroplastic TPI showed significant accumulation in response to moderate and high level of NaCl, consistent with sugar beet under 200 mM salt stress (Yang et al., 2013). In particular, MDH reversibly catalyzed the oxidation of malate to oxaloacetate and the overexpression of MDH gene enhanced the synthesis of organic acids and conferred tolerance to aluminum in transgenic alfalfa (Tesfave et al., 2001). In this study, the expression of MDH was increased under low and moderate levels of salt stress, consistent with the result of salt-treated sugar beet roots (Yang et al., 2013) and drought-treated maize (Wang et al., 2019). However, this enzyme was decreased in sugar beet (Wu et al., 2018) and upland cotton (Li et al., 2015) under salt stress conditions. A possible reason was that the MDH expression was diverse in each species under various stresses. A Calvin cycle related protein, GAPDH showed an increase in response to moderate level of NaCl. Two chloroplastic GAPDHs were accumulated in salt-treated sugar beet (Yang et al., 2013) and virus-infected Nicotiana tabacum plants (Das et al., 2019), but were depressed in drought-treated cassava (Ding et al., 2019) and salt-treated rice as well (Chitteti and Peng, 2007). PK showed increased in abundance under moderate level of salt stress, but remained unchanged under low and high ones. The results were similar between two contrasting salinity-tolerance sesame genotypes in response to salt stress (Zhang et al., 2019). Taken together, the increases of glycolysis and TCA cycle related enzymes implied the enhancement of respiration under salt stress.

In many model plants, overall carbon metabolism and the levels of sucrose and starch were severely affected under salt stress (Wang*et al.*, 2013; Zhang *et al.*, 2012), which possibly results from a metabolic shift toward sucrose production. High salinity also altered the substantial accumulation of starch grains in chloroplasts. Several proteins in this study were related to starch metabolism, such as sucrose synthase (SUS), ADP glucose pyrophosphorylase (AGP), BGLU, AMY as well as an UN (gi|661880779). We found here that AMY, an enzyme involved in the degradation of starch to sucrose, was increased, which was agreed with the metabolomics profiles that the content of sucrose was increased under severe salt stress and this would favor salt tolerance. Consistent with our result, this enzyme was induced in *Panax ginseng* leaves upon exposure to heat stress (Kim *et al.*, 2019). Particularly, an up-regulated UN (gi|661880779) is known as exhibiting hydrolase activity and also plays a role in starch and sucrose metabolism and phenylpropanoid biosynthesis (Denoeud*et al.*, 2014). Our aforementioned results demonstrated that the accumulated chloroplasts and soluble sugar were possibly employed to overcome salinity stress. After salt stress, the accumulated starch can be transformed into sucrose, which might be a consequence of a significantly up-regulated expression of the gene encoding. Furthermore, it is not noting that the most altered protein was the up-regulated chitinase with 8.6- and 9.4-fold change under moderate and high level of salt treatments, respectively. Reports showed that the up-regulated chitinase improved salt tolerance in *Thaliana* by preventing the excessive accumulation of Na⁺ (Kwon *et al.*, 2007).

However, several proteins were found to be down-regulated, such as peroxisomal (S)-2-hydroxy-acid oxidase GLO4-like isoform X5 (GLO4) under low level of salt stress, galactinol synthase 1 (GOLS1) under moderate level of salt stress and four proteins, probable rhamnose biosynthetic enzyme 1, SUS, phosphoenolpyruvate carboxykinase [ATP]-like (PCK) and an UN (gi|661898708) under high level of salt stress. Specially, GLO4 is involved in glyoxylate and dicarboxylate metabolism under salt stress (Zhang *et al.*, 2019). GOLS1, a stress-related protein, plays a key regulatory role in the carbon partitioning; overexpression of an Arabidopsis GOLS family member caused an increase in the levels of endogenous galactinol and raffinose (Taji *et al.*, 2002). In addition, the up-regulated GOLS could be found in cold-stressed *Phaseolus vulgaris* seeds (Liu *et al.*, 1998) and drought-stressed cassava (Ding *et al.*, 2019). In agreement with our research, PCK was increased in abundance in two sesame genotypes after salinity tolerance (Zhang *et al.*, 2019). Obviously, with the salt concentrations increase, the affected proteins increase to survive and adapt, supported by metabolomics results of quite high photosynthesis activity under salt stress (Chen *et al.*, 2019b).

Proteins related to energy metabolism

DEPs of ferredoxin–NADP reductase (PETH), two FBAs, alanine: glyoxylate aminotransferase isoform 1, two carbonic anhydrases (CAs), glutamine synthetase (GLN) and ferredoxin– nitrite reductase (NIR), related to energy metabolism were increased in abundance with the exception of glutamate dehydrogenase (GDH) and cysteine synthase (OASA). These DEPs were also involved in photosynthesis, carbon and nitrogen metabolisms and pentose phosphate pathway. Many studies have found that nitrogen metabolism plays an important role in the complex process of plant response to salt stress (Chen *et al.*, 2019c). Specifically, GLN functions as the major assimilatory enzyme for ammonia, and GDH works as a link between carbon and nitrogen metabolism. Therefore, the up-regulated GLN and down-regulated GDH can be a way to prevent excessive accumulation of ammonium in AVF cells, and high level of salt stress probably disturbed nitrogen transformation considering the enhanced glutamine in proteomics data (Wu *et al.*, 2018). In addition, NIR and two CAs involved in nitrogen through nitrate reduction; inconsistently, the expression of NIR homologues in salt-stressed soybean seedlings (Liu *et al.*, 2019) and drought-stressed cassava was severely inhibited (Ding *et al.*, 2019).

Photosynthesis is generally considered to be salt sensitive. PETH showed significant accumulation in response to severe salt stress, implying the adjustment of ATP synthesis, and similar result was taken place in the sugar beet (Yang *et al.*, 2013). Reports on some Calvin cycle related proteins, such as CAs, were increased in *Salicornia europaea* (Wang *et al.*, 2009) but were decreased in halophyte *Aeluropus lagopoides* (Sobhanian*et al.*, 2010) under salinity. Different species may utilize varying light reaction strategies to cope with salinity (Yu *et al.*, 2011); however, maintaining an energy supply is indispensable for plants to reduce salt stress injury. It is further supported by our proteomic results in which the levels of proteins carrying out light-dependent reactions were increased with higher salinity.

Proteins related to lipid and amino acid metabolism

Metabolic adjustments play important roles in attaining a new balance of energy and metabolites. We found that a large number of DEPs was enriched in fatty acid metabolism, linolenic acid metabolism and arachidonic acid metabolism. Four members of lipoxygenases were increased in abundance, and studies showed that the increased level of lipoxygenase 2 contributes to a protective effect against increased salinity in rice (Liu *et al.*, 2014a). Antioxidant system in lipid metabolism, including some members of ascorbate peroxidases (APXs), glutathione peroxidases (GPXs) and glutathione S-transferases (GSTs) responded to various stresses (Jiang *et al.*, 2007) was altered. Several GPX genes in Arabidopsis were up-regulated coordinately in response to stress (Rodriguez Milla *et al.*, 2003), but were down-regulated in cassava (Ding *et al.*, 2019). The flexibility and enhancement of lipid metabolism helps AVL survive under severe condition.

The iTRAQ data showed that 31 DEPs were related to a mino acid metabolism; most of them increased in abundance under low and moderate level of salt stress. Pyrroline-5-carboxylate synthetase (P5CS) is involved in the proline synthesis to overcome salt stress, and the enhanced abundance of this protein is consistent with proline content (Chen *et al.*, 2018). The up-regulated level of methionine synthase (MET) and ASP were supported by salt-stressed sugar beet (Yang*et al.*, 2013) and sesame (Zhang *et al.*, 2019), respectively.

However, several DEPs were notably inhibited under severe stress, such as 4-coumarate: CoA ligase 3 (4CL3), which can be used to synthesize several phenylpropanoid-derived compounds. Remarkably, three proteins, phenylalanine ammonia lyase (PAL), cytochrome P450 CYP73A120 (CYP) and phospho-2-dehydro-3-deoxyheptonate aldolase (aroF), were found to play important roles in alleviating the damage to plants and decreased in abundance under severe salt stress. Specifically, PAL is a key enzyme of plant metabolism based on the phenylpropane skeleton, and CYP family proteins play critical roles in flavonoid and sterol synthesis. The expression level of them was significantly suppressed under drought and salinity tolerance, respectively (Ding *et al.*, 2019; Yan *et al.*, 2014).

In addition, some DEPs related to redox system in amino acid metabolism were changed, such as CATs, APX2 and GSTs. CATs were decreased in abundance after salt stress, consistent with the physiological analysis (Chen *et al.*, 2018). Many proteomic studies have confirmed the alteration of this redox related protein (Chen *et al.*, 2019c). Known to play a crucial role in glutathione-ascorbate cycle, APX was increased in AVF under salt stress. However, the abundance of GST was regulated differently, consistent with GST6 expression in stressed maize (Zhao *et al.*, 2016). Therefore, different protein productions were adopted to alleviate damage to plants.

Proteins related to biosynthesis of secondary metabolites

A total of 23 DEPs were related to secondary metabolism. Specially, in the widely affected phenylpropanoid biosynthesis pathway, the abundance of nine proteins, including caffeic acid 3-O-methyltransferase (COMT), 4CL3, peroxidase (POD), PAL, BGLU, CYP, two cinnamyl alcohol dehydrogenases (CADs) and an UN (gi|661880779) were affected. The abundance of some proteins was exclusively suppressed under moderate or high level of salt stress, such as violaxanthin de-epoxidase, UN (gi|661892013), CAD, chalcone synthase (CHS), leucoanthocyanidin reductase 1 (LAR1), anthocyanin synthase (ANS), flavonol synthase (FLS) and UN (gi|661877099). In addition, four categories of enzymes, including CHS, chalcone isomerase (CHI), CPM and FLS, play critical roles in flavonoid synthesis under salt stress (Pi *et al.*, 2016). Besides, salt tolerance of Arabidopsis and soybean were positively regulated by CHS and negatively regulated by CHI and CPM (Pi *et al.*, 2018). In addition, alkaloid and terpenoid biosynthesis related proteins were also altered by salt. These observations were supported by the metabolomics results that more metabolic alterations were observed as the increasing levels of salt stress. Some shikimate-phenylpropanoid pathway compounds, such as flavonoids, phenolic acids and other secondary metabolites were exclusively decreased by severe salt. In short, high level of salt stress altered more DEPs related to secondary metabolite biosynthesis which probably played a crucial role in AVF response to harsh conditions.

Proteins related to signal transduction

Multiple signal transduction pathways activate other regulators, and initiate protective mechanisms through the induction or repression of functional genes to cope with salt stress (Jiang *et al.*, 2007). Most of the up-regulated proteins, such as GLN, HSPs, lactoylglutathione lyase (GLXI), GAPDH, PRH and some UNs were predominately enriched in the signal transduction pathways. In particular, the presence of CATs as well as GLXI indicates fine tuning and efficient decomposition of toxic byproducts of cellular metabolism (Wang *et al.*, 2010). Interestingly, PRH was suppressed under low level of salt stress but induced under moderate and high ones. Consistent with us, members of this family protein were suppressed by phytohormones and stress stimuli (Li *et al.*, 2015; Wang *et al.*, 2010), and regulated differently in salt-treated maize (Chen *et al.*, 2019c). Moreover, HSPs play a role in membrane stability using ROS as a signal molecule (Wang *et al.*, 2004), and the differently regulated HSPs were found in flax under heavy metal stress (Kosova *et al.*, 2011).

Proteins involved in transcription and translation

Transcriptional regulation of salt-responsive genes is a crucial part of the plant response to stress (Jiang *et al.*, 2007). RNA processing and ribonucleoprotein complex assembly may possibly represented critical processes (Lan *et al.*, 2011). In the present study, the expression level of small nuclear ribonucleoprotein associated protein B (SNRPB) was increased in low salt-treated samples, and eight RPs were increased under at least one level of salt stress. Ribosomes were showed to be essential ribonucleoprotein complexes engaged in translation (Zhang *et al.*, 2018). Observed from the proteomics results of salt-treated Arabidopsis (Jiang *et al.*, 2007) and cotton (Li*et al.*, 2015), the expression levels of some specific RPs increased while some decreased, suggesting that NaCl stress enhanced specific protein synthesis if these proteins were of particular importance to salt tolerance. In addition, eukaryotic translation initiations (eIFs) involved in protein translation (Jiang and Clouse, 2001), was observed down-regulated under low and moderate level of salt stress; similar results were found in salt-stressed Arabidopsis (Jiang *et al.*, 2007).

In addition, spliceosome proteins were down-regulated under moderate and high levels of salt stress. Published articles showed that the production of ROS and H_2O_2 triggered HSP70 synthesis and furtherly enhanced antioxidant enzyme activities (Tripathy and Oelmuller, 2012). In agreement with us, HSP70s family members regulated differently in salt-treated sugar beet (Yang *et al.*, 2013) and heat-stressed spinach (Li *et al.*, 2019).

Proteins related to folding and degradation

Proteins involved in folding and degradation play important roles in surviving from severe salt treatment. Misfolded proteins bind to chaperone BiP and are degraded through the proteasome in the disturbed homeostasis endoplasmic reticulum (Zhao *et al.*, 2016). DEPs, Glycosyltransferase (GT), dolichyldiphosphooligosaccharide (OST48), calreticulins (CRTs) and two UNs, which promoted the proper folding of proteins and prevent the aggregation of damaged proteins, were all ultimately decreased in abundance in at least one NaCl-treated sample. In particular, CPN60B and CPN60beta2 were increased in abundance in all salt-treated samples, indicating the activation of chaperones promoted by stress exposure. Notably, HSPs are often involved in assisting the folding of *de novo* synthesized polypeptides, the import/translocation of precursor proteins, preventing protein aggregation, maintaining protein functional conformation and cellular anti-stress ability (Wang *et al.*, 2004). In addition, members of other HSPs in AVF were all up-regulated in moderate levels of salt stress but remains unchanged under low one, suggesting the importance of molecular chaperones by maintaining proper protein folding and refolding for salt-tolerance.

Correlation of protein abundance and gene expression

A number of transcriptomic studies to explore genome-wide gene expression reprogramming have been done on salt stress with different species (Liu *et al.*, 2019). Under high level of salt stress, the transcript abundance was more directly relevant to the protein level. However, an overall weak correlation was in agreement with the general observation that mRNA levels do not always correlate with protein levels.

It is worth noting that in three comparisons, four DEGs/DEPs (dehydrin 1, annexin, PRH and POP) were shared in significant correlations, suggesting their crucial role under salt stress. Specifically, dehydrins are osmotically active proteins and related to stimulus response. The accumulation of dehydrin may help compensate increased Na⁺ levels in AVF, supported by the salt-treated *Hordeum vulgare* (Marsalova *et al.*, 2016). Annexin participation in diverse cellular functions highlight their essential roles in enhancing multiple stress tolerance (Yadav *et al.*, 2018). Similar to us, overexpression of annexin genes enhance tolerance in tomato (Ijaz *et al.*, 2017) and Arabidopsis (Kreps *et al.*, 2002). As mentioned above, PRH is involved in plant defense responses to several pathogens and abiotic stresses. In addition, POP is a proline-specific serine protease, and plays important roles in multiple biological processes, such as protein secretion, maturation and degradation of peptide hormones and signal transduction (Tan *et al.*, 2013). However, few reports on salt stress were found. In summary, these four proteins can be considered as targets and worth of in-depth study for improving quality engineering of this halophyte.

Molecular mechanisms revealing salt tolerance in AVF

On the basis of the identified salt-responsive proteins combined with physiology and metabolomics, we have revealed the following processes in AVF surviving from salt stress (Fig. 10). First, enhancement of photosynthesis and energy metabolism. Second, up-regulation of antioxidant enzymes. Third, accumulation of osmotic adjustments. Fourth, enhancement of secondary metabolism. At last, up-regulation of protein translation and folding. The concerted changes altogether in the above processes may provide AVF functional advantage under salt tolerance.

We realized that AVF under low level of salt stress could maintain stronger osmotic regulation ability, synergistic effects of antioxidant enzymes, energy supply capacity, signal transduction, ammonia detoxification ability as well as metabolite synthesis. The related proteins coordinate in energy metabolism and secondary metabolite biosynthesis in AVF. Furthermore, moderate and high levels of salt altered more proteins; especially the down-regulated ones related to biosynthesis of secondary metabolite. Observations also explained why the quality of low level of salt-stressed AVF was better than other samples (Chen *et al.*, 2019a; Chen *et al.*, 2019b).

CONCLUSIONS

Overall, RNA-seq based transcriptomics and the iTRAQ based proteomics of AVF were investigated under saline conditions. The purpose was to identify some salt stress responsive proteins and pathway in AVF and provided insights into the molecular mechanisms of salinity tolerance and quality formation. Results showed that the main functions of DEPs were small molecule metabolic process, biosynthetic process, response to stress as well as carbohydrate metabolic process. Furthermore, the diverse array of proteins combined with metabolomics results indicated that there was a remarkable flexibility in AVF metabolism, such as enhancement photosynthetic functions and carbohydrate metabolism under low and moderate level of salt stress and depression biosynthesis of secondary metabolites under severe stress. In addition, a weak correlation between the abundance of proteins and the corresponding transcripts demonstrated that the expression of some proteins could be regulated by post-transcriptional modifications. In general, the functional characterization of the proteins/genes revealed by integrated transcriptomics, proteomics and metabolomics will be helpful for improved understanding of the molecular mechanisms/networks in AVF and discovering new targets, and ultimately rationale engineering of halophytes with enhanced stress tolerance.

ACKNOWLEDGEMENTS

This work was supported by Priority Academic Program Development of Jiangsu Higher Education Institutions of China (NO.ysxk-2014) and Postgraduate Research & Practice Innovation Program of Jiangsu

CONFLICT OF INTEREST

Authors declare no conflict of interest.

AUTHOR CONTRIBUTIONS

C.C., W.C., and X.L. designed the experiments and managed the projects. C.C., Z.L., and Z.C. performed the experiments. Y.H., Y.M., and W.L. performed the data analysis. C.C. and X.L. wrote the manuscript.

SUPPORTING INFORMATION

Additional Supporting Information may be found online in the supporting information for this article.

Figure S1. Venn diagram analysis (A) and hierarchical clustering analysis (B) of differentially expressed metabolites of AVF exposed to salt stress compared with control.

Table S1 Specific primer pairs for qRT-PCR analysis

Table S2 Detailed information of key salt responsive DEPs

REFERENCES

Bah, A. M., Sun, H., Chen, F., Zhou, J., Dai, H., Zhang, G., & Wu, F. (2010). Comparative proteomic analysis of Typha angustifolia leaf under chromium, cadmium and lead stress. *J Hazard Mater***184** (1-3), 191-203.

Chen, C., Chen, J., Shi, J., Chen, S., Zhao, H., Yan, Y., Jiang, Y., Gu, L., Chen, F., & Liu, X. (2019). A strategy for quality evaluation of salt-treated Apocyni Veneti Folium and discovery of efficacy-associated markers by fingerprint-activity relationship modeling. *Sci Rep9* (1), 16666.

Chen, C., Liu, H., Wang, C., Liu, Z., Liu, X., Zou, L., Zhao, H., Yan, Y., Shi, J., & Chen, S. (2019). Metabolomics characterizes metabolic changes of Apocyni Veneti Folium in response to salt stress. *Plant Physiol Biochem* 144, 187-196.

Chen, C., Wang, C., Liu, Z., Liu, X., Zou, L., Shi, J., Chen, S., Chen, J., & Tan, M. (2018). Variations in Physiology and Multiple Bioactive Constituents under Salt Stress Provide Insight into the Quality Evaluation of Apocyni Veneti Folium. *Int J Mol Sci19* (10).

Chen, F., Fang, P., Peng, Y., Zeng, W., Zhao, X., Ding, Y., Zhuang, Z., Gao, Q., & Ren, B. (2019). Comparative Proteomics of Salt-Tolerant and Salt-Sensitive Maize Inbred Lines to Reveal the Molecular Mechanism of Salt Tolerance. *Int J Mol Sci* **20** (19).

Chitteti, B. R., & Peng, Z. (2007). Proteome and phosphoproteome differential expression under salinity stress in rice (Oryza sativa) roots. J Proteome Res 6 (5), 1718-1727.

Das, P. P., Lin, Q., & Wong, S. M. (2019). Comparative proteomics of Tobacco mosaic virus-infected Nicotiana tabacum plants identified major host proteins involved in photosystems and plant defence. J Proteomics 194, 191-199.

de Abreu, C. E., Araujo Gdos, S., Monteiro-Moreira, A. C., Costa, J. H., Leite Hde, B., Moreno, F. B., Prisco, J. T., & Gomes-Filho, E. (2014). Proteomic analysis of salt stress and recovery in leaves of Vigna unguiculata cultivars differing in salt tolerance. *Plant Cell Rep33* (8), 1289-1306.

Denoeud, F., Carretero-Paulet, L., Dereeper, A., Droc, G., Guyot, R., Pietrella, M., Zheng, C., Alberti, A., Anthony, F., Aprea, G., Aury, J. M., Bento, P., Bernard, M., Bocs, S., Campa, C., Cenci, A., Combes,

M. C., Crouzillat, D., Da Silva, C., Daddiego, L., De Bellis, F., Dussert, S., Garsmeur, O., Gayraud, T., Guignon, V., Jahn, K., Jamilloux, V., Joet, T., Labadie, K., Lan, T., Leclercq, J., Lepelley, M., Leroy, T., Li, L. T., Librado, P., Lopez, L., Munoz, A., Noel, B., Pallavicini, A., Perrotta, G., Poncet, V., Pot, D., Priyono, Rigoreau, M., Rouard, M., Rozas, J., Tranchant-Dubreuil, C., VanBuren, R., Zhang, Q., Andrade, A. C., Argout, X., Bertrand, B., de Kochko, A., Graziosi, G., Henry, R. J., Jayarama, Ming, R., Nagai, C., Rounsley, S., Sankoff, D., Giuliano, G., Albert, V. A., Wincker, P., & Lashermes, P. (2014). The coffee genome provides insight into the convergent evolution of caffeine biosynthesis. *Science* **345** (6201), 1181-1184.

Dietz, K. J., Sauter, A., Wichert, K., Messdaghi, D., & Hartung, W. (2000). Extracellular beta-glucosidase activity in barley involved in the hydrolysis of ABA glucose conjugate in leaves. *J Exp Bot***51** (346), 937-944.

Ding, Z., Fu, L., Tie, W., Yan, Y., Wu, C., Hu, W., & Zhang, J. (2019). Extensive Post-Transcriptional Regulation Revealed by Transcriptomic and Proteomic Integrative Analysis in Cassava under Drought. J Agric Food Chem 67 (12), 3521-3534.

Flowers, T. J. (2004). Improving crop salt tolerance. J Exp Bot55 (396), 307-319.

Hua, Y., Wang, S., Liu, Z., Liu, X., Zou, L., Gu, W., Hou, Y., Ma, Y., Luo, Y., & Liu, J. (2016). iTRAQbased quantitative proteomic analysis of cultivated Pseudostellaria heterophylla and its wild-type. *J Proteomics* 139, 13-25.

Ijaz, R., Ejaz, J., Gao, S., Liu, T., Imtiaz, M., Ye, Z., & Wang, T. (2017). Overexpression of annexin gene AnnSp2, enhances drought and salt tolerance through modulation of ABA synthesis and scavenging ROS in tomato. *Sci Rep* **7** (1), 12087.

Jiang, J., & Clouse, S. D. (2001). Expression of a plant gene with sequence similarity to animal TGF-beta receptor interacting protein is regulated by brassinosteroids and required for normal plant development. *Plant J* **26** (1), 35-45.

Jiang, Y., Yang, B., Harris, N. S., & Deyholos, M. K. (2007). Comparative proteomic analysis of NaCl stress-responsive proteins in Arabidopsis roots. *J Exp Bot* 58 (13), 3591-3607.

Kim, S. W., Gupta, R., Min, C. W., Lee, S. H., Cheon, Y. E., Meng, Q. F., Jang, J. W., Hong, C. E., Lee, J. Y., Jo, I. H., & Kim, S. T. (2019). Label-free quantitative proteomic analysis of Panax ginseng leaves upon exposure to heat stress. *J Ginseng Res43* (1), 143-153.

Kosova, K., Vitamvas, P., Prasil, I. T., & Renaut, J. (2011). Plant proteome changes under abiotic stresscontribution of proteomics studies to understanding plant stress response. *J Proteomics***74** (8), 1301-1322.

Kreps, J. A., Wu, Y., Chang, H.-S., Zhu, T., Wang, X., & Harper, J. F. (2002). Transcriptome Changes for Arabidopsis in Response to Salt, Osmotic, and Cold Stress. *Plant Physiology* **130** (4), 2129-2141.

Kwon, Y., Kim, S. H., Jung, M. S., Kim, M. S., Oh, J. E., Ju, H. W., Kim, K. I., Vierling, E., Lee, H., & Hong, S. W. (2007). Arabidopsis hot2 encodes an endochitinase-like protein that is essential for tolerance to heat, salt and drought stresses. *Plant J49* (2), 184-193.

Lan, P., Li, W., Wen, T. N., Shiau, J. Y., Wu, Y. C., Lin, W., & Schmidt, W. (2011). iTRAQ protein profile analysis of Arabidopsis roots reveals new aspects critical for iron homeostasis. *Plant Physiol*155 (2), 821-834.

Li, Q., Li, P., Sun, L., Wang, Y., Ji, K., Sun, Y., Dai, S., Chen, P., Duan, C., & Leng, P. (2012). Expression analysis of beta-glucosidase genes that regulate abscisic acid homeostasis during watermelon (Citrullus lanatus) development and under stress conditions. *J Plant Physiol* **169** (1), 78-85.

Li, S., Yu, J., Li, Y., Zhang, H., Bao, X., Bian, J., Xu, C., Wang, X., Cai, X., Wang, Q., Wang, P., Guo, S., Miao, Y., Chen, S., Qin, Z., & Dai, S. (2019). Heat-Responsive Proteomics of a Heat-Sensitive Spinach Variety. *Int J Mol Sci* 20 (16).

Li, W., Wei, Z., Qiao, Z., Wu, Z., Cheng, L., & Wang, Y. (2013). Proteomics analysis of alfalfa response to heat stress. *PLoS One*8 (12), e82725-e82725.

Li, W., Zhao, F., Fang, W., Xie, D., Hou, J., Yang, X., Zhao, Y., Tang, Z., Nie, L., & Lv, S. (2015). Identification of early salt stress responsive proteins in seedling roots of upland cotton (Gossypium hirsutum L.) employing iTRAQ-based proteomic technique. *Front Plant Sci* **6**, 732.

Liu, A., Xiao, Z., Li, M. W., Wong, F. L., Yung, W. S., Ku, Y. S., Wang, Q., Wang, X., Xie, M., Yim, A. K., Chan, T. F., & Lam, H. M. (2019). Transcriptomic reprogramming in soybean seedlings under salt stress. *Plant Cell Environ* 42 (1), 98-114.

Liu, C. W., Chang, T. S., Hsu, Y. K., Wang, A. Z., Yen, H. C., Wu, Y. P., Wang, C. S., & Lai, C. C. (2014). Comparative proteomic analysis of early salt stress responsive proteins in roots and leaves of rice. *Proteomics* 14 (15), 1759-1775.

Liu, G. T., Ma, L., Duan, W., Wang, B. C., Li, J. H., Xu, H. G., Yan, X. Q., Yan, B. F., Li, S. H., & Wang, L. J. (2014). Differential proteomic analysis of grapevine leaves by iTRAQ reveals responses to heat stress and subsequent recovery. *BMC Plant Biol* 14, 110.

Liu, J. J. J., Krenz, D. C., Galvez, A. F., & Lumen, B. O. D. (1998). Galactinol synthase (GS): Increased enzyme activity and levels of mRNA due to cold and desiccation. *Plant Science* 134 (1), 11-20.

Marsalova, L., Vitamvas, P., Hynek, R., Prasil, I. T., & Kosova, K. (2016). Proteomic Response of Hordeum vulgare cv. Tadmor and Hordeum marinum to Salinity Stress: Similarities and Differences between a Glycophyte and a Halophyte. *Front Plant Sci* **7**, 1154.

Mooney, B. P., Miernyk, J. A., Greenlief, C. M., & Thelen, J. J. (2006). Using quantitative proteomics of Arabidopsis roots and leaves to predict metabolic activity. *Physiol Plant* **128** (2), 237-250.

Pi, E., Qu, L., Hu, J., Huang, Y., Qiu, L., Lu, H., Jiang, B., Liu, C., Peng, T., Zhao, Y., Wang, H., Tsai, S. N., Ngai, S., & Du, L. (2016). Mechanisms of Soybean Roots' Tolerances to Salinity Revealed by Proteomic and Phosphoproteomic Comparisons Between Two Cultivars. *Mol Cell Proteomics* 15 (1), 266-288.

Pi, E., Zhu, C., Fan, W., Huang, Y., Qu, L., Li, Y., Zhao, Q., Ding, F., Qiu, L., Wang, H., Poovaiah, B. W., & Du, L. (2018). Quantitative Phosphoproteomic and Metabolomic Analyses Reveal GmMYB173 Optimizes Flavonoid Metabolism in Soybean under Salt Stress. *Mol Cell Proteomics* **17** (6), 1209-1224.

Pu, Y., Walley, J. W., Shen, Z., Lang, M. G., Briggs, S. P., Estelle, M., & Kelley, D. R. (2019). Quantitative Early Auxin Root Proteomics Identifies GAUT10, a Galacturonosyltransferase, as a Novel Regulator of Root Meristem Maintenance. *Mol Cell Proteomics* 18 (6), 1157-1170.

Rodriguez Milla, M. A., Maurer, A., Rodriguez Huete, A., & Gustafson, J. P. (2003). Glutathione peroxidase genes in Arabidopsis are ubiquitous and regulated by abiotic stresses through diverse signaling pathways.*Plant J* **36** (5), 602-615.

Sobhanian, H., Motamed, N., Jazii, F. R., Nakamura, T., & Komatsu, S. (2010). Salt Stress Induced Differential Proteome and Metabolome Response in the Shoots of Aeluropus lagopoides (Poaceae), a Halophyte C-4 Plant. *Journal of Proteome Research* **9** (6), 2882-2897.

Stanley Kim, H., Yu, Y., Snesrud, E. C., Moy, L. P., Linford, L. D., Haas, B. J., Nierman, W. C., & Quackenbush, J. (2005). Transcriptional divergence of the duplicated oxidative stress-responsive genes in the Arabidopsis genome. *Plant J* **41** (2), 212-220.

Taji, T., Ohsumi, C., Iuchi, S., Seki, M., Kasuga, M., Kobayashi, M., Yamaguchi-Shinozaki, K., & Shinozaki, K. (2002). Important roles of drought- and cold-inducible genes for galactinol synthase in stress tolerance in Arabidopsis thaliana. *Plant J* **29** (4), 417-426.

Tan, C. M., Chen, R. J., Zhang, J. H., Gao, X. L., Li, L. H., Wang, P. R., Deng, X. J., & Xu, Z. J. (2013). OsPOP5, a prolyl oligopeptidase family gene from rice confers abiotic stress tolerance in Escherichia coli. Int J Mol Sci 14 (10), 20204-20219.

Tesfaye, M., Temple, S. J., Allan, D. L., Vance, C. P., & Samac, D. A. (2001). Overexpression of malate dehydrogenase in transgenic alfalfa enhances organic acid synthesis and confers tolerance to aluminum. *Plant Physiol* **127** (4), 1836-1844.

Tripathy, B. C., & Oelmuller, R. (2012). Reactive oxygen species generation and signaling in plants. *Plant Signal Behav***7** (12), 1621-1633.

Wang, L., Liang, W., Xing, J., Tan, F., Chen, Y., Huang, L., Cheng, C. L., & Chen, W. (2013). Dynamics of chloroplast proteome in salt-stressed mangrove Kandelia candel (L.) Druce. *J Proteome Res12* (11), 5124-5136.

Wang, W., Vinocur, B., Shoseyov, O., & Altman, A. (2004). Role of plant heat-shock proteins and molecular chaperones in the abiotic stress response. *Trends Plant Sci* **9** (5), 244-252.

Wang, X., Fan, P., Song, H., Chen, X., Li, X., & Li, Y. (2009). Comparative proteomic analysis of differentially expressed proteins in shoots of Salicornia europaea under different salinity. *J Proteome Res* 8 (7), 3331-3345.

Wang, X., Tang, C., Deng, L., Cai, G., Liu, X., Liu, B., Han, Q., Buchenauer, H., Wei, G., Han, D., Huang, L., & Kang, Z. (2010). Characterization of a pathogenesis-related thaumatin-like protein gene TaPR5 from wheat induced by stripe rust fungus. *Physiol Plant139* (1), 27-38.

Wang, X., Zenda, T., Liu, S., Liu, G., Jin, H., Dai, L., Dong, A., Yang, Y., & Duan, H. (2019). Comparative Proteomics and Physiological Analyses Reveal Important Maize Filling-Kernel Drought-Responsive Genes and Metabolic Pathways. *Int J Mol Sci* **20** (15).

Wu, G. Q., Wang, J. L., Feng, R. J., Li, S. J., & Wang, C. M. (2018). iTRAQ-Based Comparative Proteomic Analysis Provides Insights into Molecular Mechanisms of Salt Tolerance in Sugar Beet (Beta vulgaris L.). *Int J Mol Sci* 19 (12).

Xie, W., Zhang, X., Wang, T., & Hu, J. (2012). Botany, traditional uses, phytochemistry and pharmacology of Apocynum venetum L. (Luobuma): A review. *J Ethnopharmacol* 141 (1), 1-8.

Yadav, D., Boyidi, P., Ahmed, I., & Kirti, P. B. (2018). Plant annexins and their involvement in stress responses. *Environmental and Experimental Botany* 155, 293-306.

Yan, J., Wang, B., Jiang, Y., Cheng, L., & Wu, T. (2014). GmFNSII-controlled soybean flavone metabolism responds to abiotic stresses and regulates plant salt tolerance. *Plant Cell Physiol*55 (1), 74-86.

Yang, L., Zhang, Y., Zhu, N., Koh, J., Ma, C., Pan, Y., Yu, B., Chen, S., & Li, H. (2013). Proteomic analysis of salt tolerance in sugar beet monosomic addition line M14. *J Proteome Res* 12 (11), 4931-4950.

Yu, J., Chen, S., Zhao, Q., Wang, T., Yang, C., Diaz, C., Sun, G., & Dai, S. (2011). Physiological and proteomic analysis of salinity tolerance in Puccinellia tenuiflora. *J Proteome Res10* (9), 3852-3870.

Zhang, A., Han, D., Wang, Y., Mu, H., Zhang, T., Yan, X., & Pang, Q. (2018). Transcriptomic and proteomic feature of salt stress-regulated network in Jerusalem artichoke (Helianthus tuberosus L.) root based on de novo assembly sequencing analysis. *Planta* **247** (3), 715-732.

Zhang, H., Han, B., Wang, T., Chen, S., Li, H., Zhang, Y., & Dai, S. (2012). Mechanisms of plant salt response: insights from proteomics. *J Proteome Res* 11 (1), 49-67.

Zhang, Y., Wei, M., Liu, A., Zhou, R., Li, D., Dossa, K., Wang, L., Zhang, Y., Gong, H., Zhang, X., & You, J. (2019). Comparative proteomic analysis of two sesame genotypes with contrasting salinity tolerance in response to salt stress. *J Proteomics* **201**, 73-83.

Zhao, F., Zhang, D., Zhao, Y., Wang, W., Yang, H., Tai, F., Li, C., & Hu, X. (2016). The Difference of Physiological and Proteomic Changes in Maize Leaves Adaptation to Drought, Heat, and Combined Both Stresses. *Front Plant Sci* **7**, 1471.

Figure legends

Figure 1. Generalized workflow combining the strengths of transcriptome, proteome, metabolome and physiology analyses for the study of salt tolerance of AVF and revealing the mechanism of quality formation. Transcriptomics and proteomics were applied to identify the proteins in different levels of salt-stressed AVF. After GO, KEGG and STRING analysis, DEPs played important roles in response to salt stress combined with physiology and metabolomics analysis in our previous reports to revealed the mechanisms of salt tolerance and quality formation of AVF.

Figure 2. Summary of the iTRAQ information. Bar charts showed the peptide length distribution (A), isoelectric distribution (B), peptide number distribution (C), distribution of proteins' sequences coverage (D) and a pie chart represented the percentage for protein mass distribution (E).

Figure 3. Overview of the DEPs in salt-stressed AVF compared to the control. Venn diagram showed the number of proteins with significant expression changes in AVF exposed to different levels of salt compared with control (A). Histograms revealed the up and down DEPs in salt-treated plants compared with control (B). Functional classification of the DEPs (C).

Figure 4. KEGG pathway of the DEPs in AVF exposed to different levels of salt compared to the control.

Figure 5. The protein–protein interaction network of the DEPs in AVF exposed to low, moderate and high levels of salt stress compared to the control, respectively. DEPs with strong interactions were marked within the red oval.

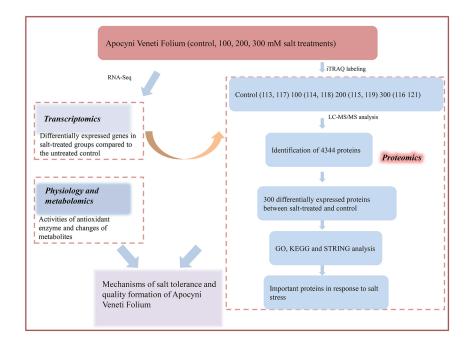
Figure 6. Overview of the shared DEPs in salt-treated AVF samples compared to the control. Heat map (A), molecular function (B), biological process (C), KEGG pathway analysis (D) and protein-protein interaction (E).

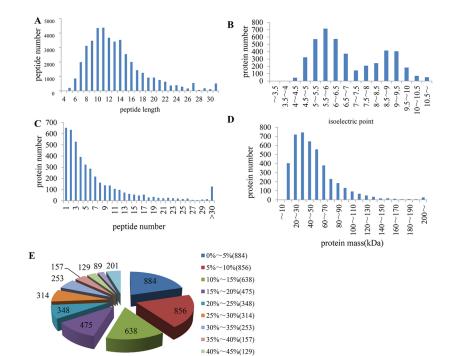
Figure 7. Relative abundances of salt responsive proteins compared with control in AVF revealed by qRT-PCR. (A) Ferritin (Pr_AVENL_17965_1); (B) uncharacterized protein (Pr_AVENL_20218_1); (C) ATP synthase subunit delta, chloroplastic (Pr_AVENL_23089_1); (D) uncharacterized protein (Pr_AVENL_25878_-1); (E) hypothetical protein B456_003G066700 (Pr_AVENL_27306_1); (F) ruBisCO large subunit-binding protein subunit beta, chloroplastic (Pr_AVENL_3558_1); (G) catalase (Pr_AVENL_4882_1); (H) pathogenesis related protein (Pr_AVENL_23055_1); (I) dehydrin 1 (Pr_AVENL_972_1). Bars represent mean +- SE (n = 3). Differences were evaluated by unpaired Student's t-test at 0.05 level.

Figure 8. Gene expression levels using RNA-seq and qRT-PCR in AVF under different levels of salt stress compared with control.

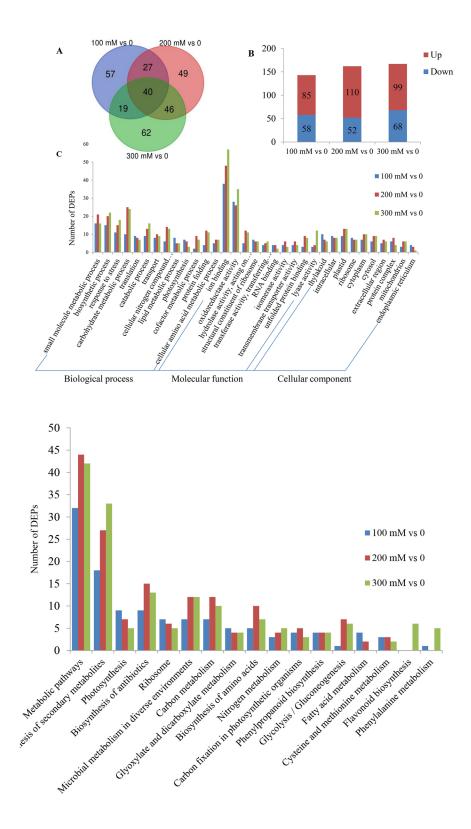
Figure 9. Correlation between transcripts and proteins in AVF under different levels of salt stress compared with control. A, 100 mM vs 0; B, 200 mM vs 0; C, 300 mM vs 0; D, salt treatment vs 0, respectively. rho, correlation coefficient between DEGs and their corresponding DEPs.

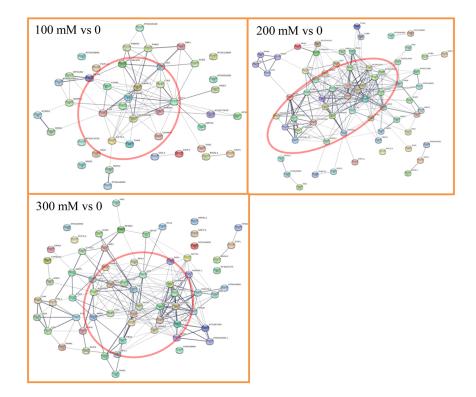
Figure 10. Molecular models of salt tolerance in different levels of salt-stressed AVF based on proteomics. Protein expression patterns under salt stress were shown by marking the proteins in red for up-regulated proteins and in green for down-regulated proteins in heat maps.

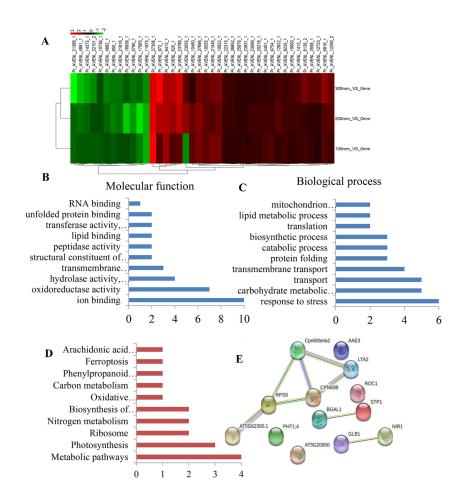


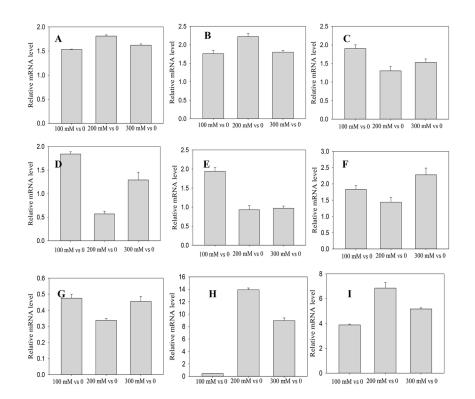


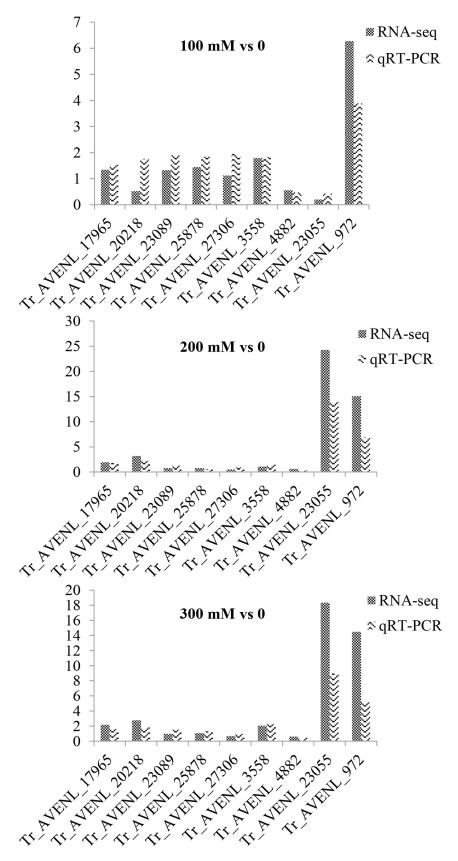
■ 45%~50%(89) ■ 50%~100%(201)

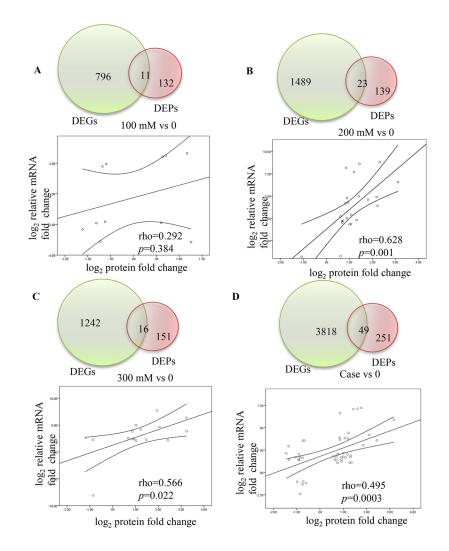












P. AVESL, 994, 1 P. AVESL, 203 J P. AVESL, 203 J P. AVESL, 407 J P. AVESL, 407 J P. AVESL, 407 J	100 mM/rs 0 200 mJ cell redox homeostasis		n Artist, 279(1) p.Artist, 499(1) p.Artist, 499(1) p.Artist, 249(1) p.Artist, 24	Pr, AVENL, 1915.2 Pr, AVENL, 1915.2 Pr, AVENL, 2284.1 Pr, AVENL, 2284.1 Pr, AVENL, 2284.1 Pr, AVENL, 2284.1 Pr, AVENL, 2387.1 Pr, AVENL, 2387.1
Pr_AVENL_10752_1 Pr_AVENL_14532_1 Pr_AVENL_4880_1 Pr_AVENL_4882_1	hydrogen peroxide catabolic process		carbohydrate metabolic process	P: AVEN13111 P: AVEN11607_1 P: AVEN23136_1 P: AVEN4338_1 P: AVEN4338_1 P: AVEN12708_1
Pr, AVENL, 27503, 2 Pr, AVENL, 1749, J Pr, AVENL, 1449, J Pr, AVENL, 1546, J Pr, AVENL, 1545, J Pr, AVENL, 1645, J Pr, AVENL, 1165, J Pr, AVENL, 1165, J Pr, AVENL, 2165, J	protein folding and refolding		photosynthesis	P. AVENL, 16695.1 P. AVENL, 9452.1 P. AVENL, 9452.1 P. AVENL, 16213.3 P. AVENL, 16213.1 P. AVENL, 1513.1 P. AVENL, 1514.1 P. AVENL, 1514.1 P. AVENL, 1514.1 P. AVENL, 1514.1 P. AVENL, 1514.1 P. AVENL, 1514.1
Pr_AVENL_2215_1 Pr_AVENL_2325_1 Pr_AVENL_2359_1 Pr_AVENL_2439_1 Pr_AVENL_24499_1 Pr_AVENL_161911		Salt stress	nitrogen metabolism	Pr_AVENL_9754_1 Pr_AVENL_24500_1
P_AVENL_27181_2 Pr_AVENL_27181_2 Pr_AVENL_5558_1 Pr_AVENL_620_1			lipid metabolic process	Pr_AVENL_18236_1 Pr_AVENL_21583_1 Pr_AVENL_21589_1 Pr_AVENL_21596_1 Pr_AVENL_21596_1 Pr_AVENL_14604_1 Pr_AVENL_16007_1
Pr_AVENL_972_1	stress and defense			Pr_AVENL_19701_1 Pr_AVENL_9754_1
P AVES 141 P AVES	transcription and translation		amino acid biosynthetic and metabolic process condary metabolite	P. AVEN_4467 1 P. AVEN_4467 1 P. AVEN_7007 1 P. AVEN_1476 1 P. AVEN_421 3 P. AVEN_2031 1 P. AVEN_2033 1 P. AVEN_2034 1 P. AVEN
	20100 U2018340001 P ₁ AV882[491] P ₁ AV882[491]		osynthetic process	A AND A 1998 (1 A 100 (1) (1) (1) (1) (1) (1) (1) (1) (1) (1)